



Universiteit  
Leiden  
The Netherlands

## **Absolute photometry of the supernova remnants N 49 and N 63 A in the Large Magellanic Cloud**

Greve, A.; Genderen, A.M. van

### **Citation**

Greve, A., & Genderen, A. M. van. (1977). Absolute photometry of the supernova remnants N 49 and N 63 A in the Large Magellanic Cloud. *Astronomy And Astrophysics*, 59, 267-272.  
Retrieved from <https://hdl.handle.net/1887/7087>

Version: Not Applicable (or Unknown)

License: [Leiden University Non-exclusive license](#)

Downloaded from: <https://hdl.handle.net/1887/7087>

**Note:** To cite this publication please use the final published version (if applicable).

## Absolute Photometry of the Supernova Remnants N 49 and N 63A in the Large Magellanic Cloud

A. Greve<sup>1</sup> and A. M. van Genderen<sup>2</sup>

<sup>1</sup> Max-Planck-Institut für Radioastronomie, Auf dem Hügel 69, D-5300 Bonn, Federal Republic of Germany

<sup>2</sup> Leiden Southern Station, Broederstroom, Rep. South Africa

Received August 5, 1976; revised February 28, 1977

**Summary.** We present five-colour photometric (Walraven system) observations of the supernova remnants N 49 and N 63 A of the Large Magellanic Cloud. The observations of N 49 indicate an optically thin, filamentary shell. The photometric observations allow a calibration of the spectroscopic observations of N 49, published by Osterbrock and Dufour (1973); absolute surface intensities of the spectral lines can be derived.

A detailed comparison of the observations of N 49 with predictions from shock wave models is made and good agreement is found. As a particular conclusion, the interstellar medium density near N 49 is found to be  $13 \text{ cm}^{-3}$ .

**Key words:** supernova remnants — photometry — absolute spectral line intensities — shock wave model

### Introduction

Because of their non-thermal radio and optical emission line spectra, the nebulae N 49 and N 63 A (Henize's catalog, 1956) of the Large Magellanic Cloud (LMC) are identified by Westerlund and Mathewson (1966, abbreviated WM), and Mathewson and Clarke (1973, MC) as supernova remnants (SNR) of Type II. Stimulated by WM's investigation we made five-colour photometric observations of both nebulae, once of the integrated objects and secondly along particular scans across the emission features. These observations (I), in particular those of N 49, allow us to investigate the geometrical structure of the objects (II), to determine the amount of radiated optical energy (III), and to make a detailed comparison with predictions from shock wave models (IX).

### I. The Observations and Reductions

The observations were made with the Walraven five-colour simultaneous photometer attached to the 90 cm light collector of the Leiden Southern Station (at the

SAAO annexe) in South Africa. The effective wavelengths of the *V*, *B*, *L*, *U*, *W* pass bands are roughly 5467 Å, 4325 Å, 3838 Å, 3633 Å, 3255 Å, respectively. A description of the photometer and the photometric system is given by Walraven and Walraven (1960), Rijn et al. (1969) and Lub and Pel (1977).

A number of observations were obtained in 1966, in particular those made with the diaphragm of 65" diameter which is comparable with the diameter of the SNR of 67" and 27" (WM) at  $H_{\alpha}$  for N 49 and N 63 A, respectively. The brightness and the colours in the Walraven system were derived from comparison with at least five Walraven standard stars; the sky background measurements were taken in nearby regions. Because of the crowding of stars in the 65" field some faint stars are included in the measurements, however, their influence on the total brightness and the total colour are estimated to be negligible small. In Table 1 we list the 1966 observations of the integrated objects.

In 1971, both nebulae were scanned with a 16" diameter diaphragm. N 49 was scanned in steps of 15" in RA and  $\delta$ , while for the central parts of N 49 the steps were reduced to 7.5" in RA. N 63 A was scanned in steps of 7.5" in RA and  $\delta$ . This procedure was facilitated by an illuminated grid, of which the squares have dimensions of 15", in the eyepiece and a few nearby stars bright enough to be used as offset stars. The usual integration time for one measurement was 90 and 120 s. After having finished one scan in RA, a sky measurement was made in a nearby, fixed region of the sky. Regularly, HD 33579, a standard star of the Walraven system and a member of

**Table 1.** Five-colour photometric observations (Walraven system) of N 49 and N 63 A, made with a 65" diaphragm centered on the nebulae. Given are log intensity, the sky back ground is subtracted. Integration time N 49: 180 s, N 63 A: 120 s, not reduced

Object	<i>V</i>	<i>V</i> – <i>B</i>	<i>B</i> – <i>U</i>	<i>U</i> – <i>W</i>	<i>B</i> – <i>L</i>
N 49	–2.315	0.127	–0.398	0.501	–0.394
N 63 A	–2.758	0.020	–0.235	0.271	–0.188

Send offprint requests to: A. Greve

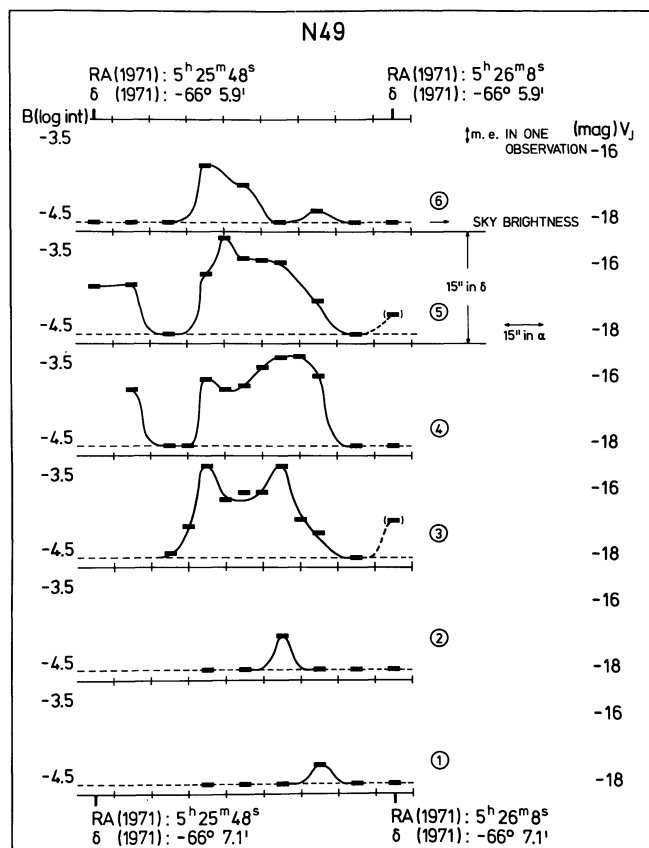


Fig. 1.  $B$  pass band (Walraven five-colour system, effective wavelength  $4325 \text{ \AA}$ ) observations of N49. The bars indicate positions at which measurements are made, the solid lines give an approximation of the intensity variation. North is at the top, east at the right hand side. The vertical scale at the left hand side gives log intensity in the  $B$  pass band; the vertical scale at the right hand side gives  $V$  of the  $UBV$  system as an indication of the magnitude of the object

the LMC, was measured as a comparison star. Twice during the program, five standard stars were measured to obtain the extinction coefficients. Most of the scans, especially those of the brightest parts of the nebulae, were repeated two or three times to give the mean error of one measurement, i.e. in the  $B$  pass band this gives 0.1 in log intensity, equal to 0.25 mag.

Some difficulties arose when it became clear that the comparison star HD 33579 is a slightly variable star (Walraven and Walraven, 1971; Rosendahl and Snowden, 1971). Therefore, HD 33579 was regularly observed to obtain its brightness variation. We found that the total light variability is smaller than 0.1 m with a time scale of a few months (van Genderen, 1974), however, the brightness and colours of HD 33579, derived from the five standard stars, observed during the SNR program were sufficiently accurate for comparison.

In Figure 1 and 2 we show the scans in the representative,  $B$  pass band for N49 and N63 A, respectively. The vertical scales at the left hand side give log intensity in the  $B$  pass band. At the positions of the observations a heavy bar is drawn in Figures 1 and 2; the

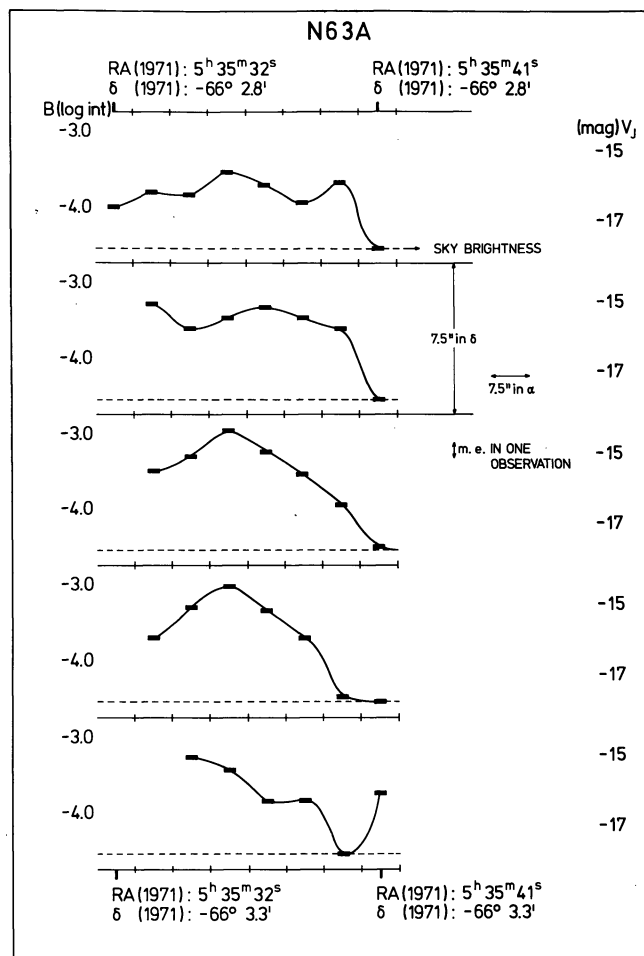


Fig. 2.  $B$  pass band (Walraven five-colour system, effective wavelength  $4325 \text{ \AA}$ ) observations of N63 A. The bars indicate positions at which measurements are made, the solid lines give an approximation of the intensity variation. North is at the top, east at the right hand side. The vertical scale at the left hand side gives log intensity in the  $B$  pass band; the vertical scale at the right hand side gives  $V$  of the  $UBV$  system as an indication of the magnitude of the object

solid lines drawn through these points give an approximation of the positional variation of the intensity. On the western side (left hand side, Fig. 2) of N63 A, field stars disturbed the scans; as soon as a field star entered the diaphragm the scan was terminated.

The co-ordinates of observation are accurate to  $2''$  in RA,  $0.2$  in  $\delta$ .

Figure 3 shows a photograph of N49 in the blue light, onto which the intensity distribution of the  $B$  pass band, shown in Figure 1, is superimposed. Some field stars, disturbing the scans, are indicated by asterisks.

## II. Geometrical Structure

### N49.

A detailed morphological description, based on radio and optical observations, of the objects within an area of  $17'$  diameter, centered on N49, is given by MC (1973a). Figure 3 shows N49 as a filamentary shell, broken up in

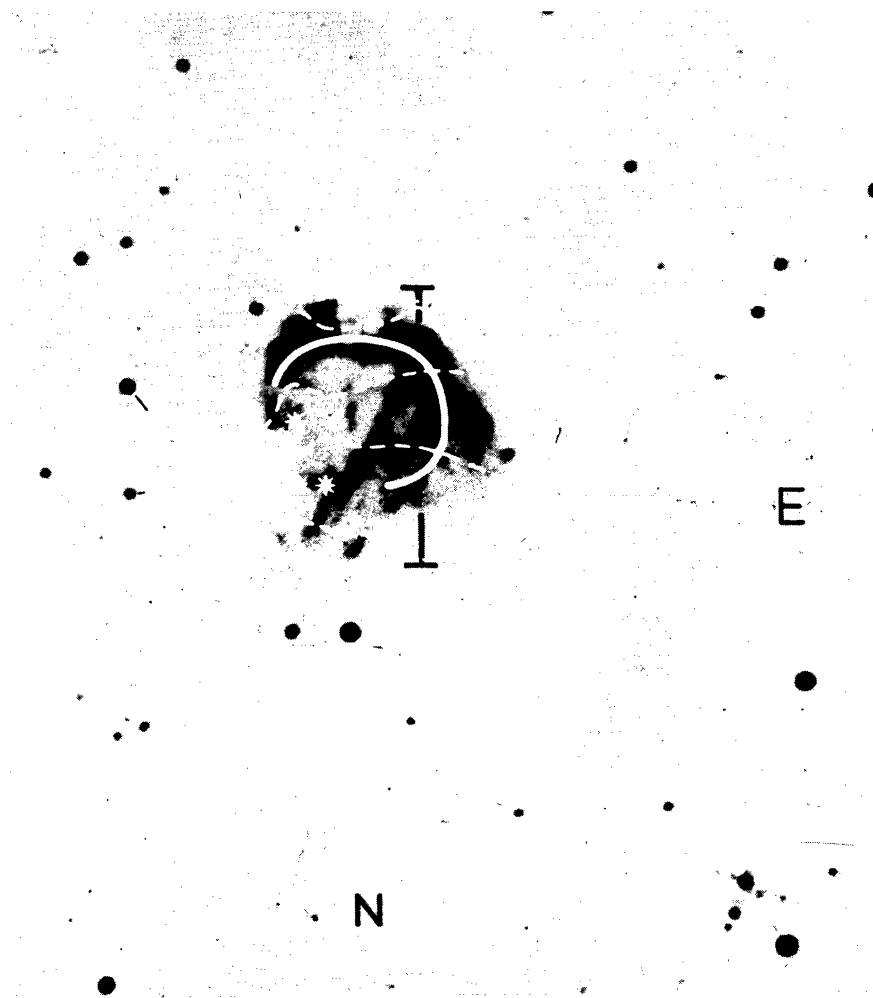


Fig. 3. Photograph of N49 taken in the blue light. The length of the bar indicates 1 min of arc. Overlay of the photometric scans (*B* pass band) shown in Figure 1. The ridge of the shell is indicated by the solid arc. The asterisks indicate disturbing field stars

the direction NW which is away from the high density region of the LMC (WM 1966). This disruption of the shell suggests the ejection of the radio source 0525-660 from the SNR. With 55 kpc as the distance of the LMC, the diameter of the shell is 16 pc, the thickness of the filaments is 4 pc (MC 1973).

The shell like structure is clearly indicated by the scans shown in Figure 1, in particular by scan No. 3; in the overlay picture Figure 3, this scan is indicated by the arrow. The scan passing the center, No. 4 of Figure 1 and marked *C* in Figure 3, is less indicative because of the gap in the shell and the influence of a field star. For the *V*, *B*, *L*, *U* pass bands, in Figure 4 we show scan No. 3 on a linear scale of absolute surface intensities; this intensity distribution is typical of an optically thin shell.

Therefore, assuming that the source function  $S(\nu)$  is constant throughout the emitting shell of thickness  $d$ , the surface intensity  $J(\nu)$  is given by

$$J(\nu) = S(\nu)(1 - e^{-\tau(\nu)}) \approx S(\nu)\tau(\nu) \quad (1)$$

with  $\tau(\nu) = \chi(\nu)d$ ,  $\chi(\nu)$  being the absorption coefficient. For two, highly idealized geometrical models of the shell

Model I :  $R = 8$  pc,  $r = 4$  pc,

Model II:  $R = 8$  pc,  $r = 6$  pc

( $R$  = outer radius,  $r$  = inner radius of the shell) we calculated  $d$  as a function of the apparent radial distance  $D$ , from which in turn we calculated, using Equation (1), the surface intensities  $J(I, D)$  and  $J(II, D)$ , normalized to  $J(D=0) = 1$ . The intensity distributions  $J(I)$ ,  $J(II)$  are shown in Figure 5 together with the observed intensities of the *U*, *V* pass bands. Considering the angular resolution of the observation ( $7.5''$ ), the western part and the eastern part of the shell, at least for the intensity of the *U* pass band, is represented by Model I, while for the eastern part the intensity of the *V* pass band is represented by a model in between I and II, i.e.  $R = 8$  pc,  $r \approx 5$  pc. These values agree well with those given by MC, while the spatial intensity distribution confirms the assumption of an optically thin shell.

#### N63 A

According to WMs' optical observations, N63 A shows three bright concentrations extending starlike from the center of the nebula. The diameter of the shell is 7 pc, the thickness of the filaments is 2.5 pc (MC), which, however, is a highly idealized geometrical picture. Considering the angular resolution of the observations, Figure 2 suggests

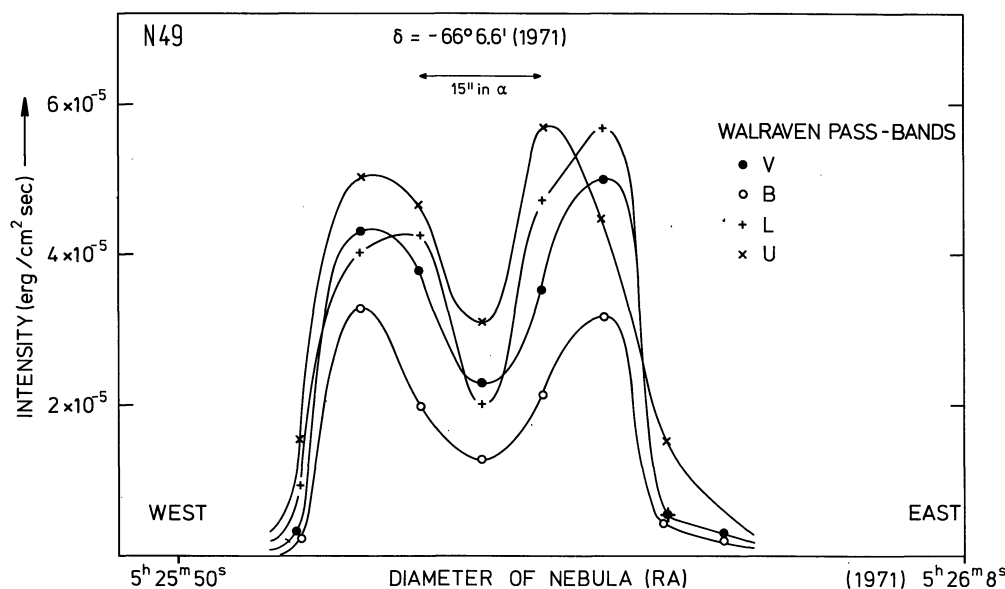


Fig. 4. N49, scan No. 3 (Fig. 1) shown in absolute surface intensities. The symbols indicate positions at which measurements are taken. The intensity distribution is typical of an optically thin shell

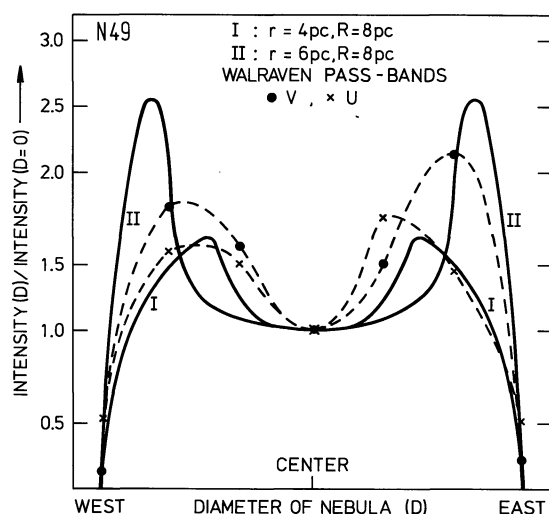


Fig. 5. N49. Comparison of the observations and the predicted intensity distribution of two Models (I, II) of an optically thin shell

a compact object with no clear indication of a shell like structure. However, on the western side the observations are incomplete because of disturbing field stars. Furthermore, the nebula may be optically thick so that the shell structure is masked by this effect.

### III. Emitted Optical Energy (N49)

The absolute nebular surface intensities, weighted with the filter pass bands, are obtained by comparing the absolute solar intensities transmitted in the pass bands [derived from the Walraven colours of a G2V main sequence star and by convolving the absolute solar surface intensity, taken from Allen (1973) with the filter functions] with the observed nebular intensities. The

basic observations for the integrated objects are those given in Table 1. We have chosen  $R(N49)=8$  pc,  $R(N63A)=7$  pc, together with a filling factor  $1/3$  for N49, and  $1/2$  for N63A to take into account the filamentary structure of the nebulae. The filling factors are somewhat uncertain, they are indicated by the optical appearance of the nebulae (WM 1966). In Table 2 we list the resulting surface intensities; we find that, averaged for the integrated objects, N63A is about 4 times brighter than N49.

For the south-east ridge of N49, detailed spectroscopic observations (line identifications and relative line intensities) are published by Osterbrock and Dufour (1973, OD). The observations by Danziger and Dennefeld give qualitative descriptions of the spectra (1976) and eye estimates of line strengths (1974) which, however, do not allow quantitative interpretations.

We relate ODs' observation of the south-east ridge, coinciding with the shell, to the particular observation of our set which covers nearly the same region. The spectral region  $3727-6731 \text{ \AA}$  analyzed by OD covers the Walraven  $V, B$  pass bands. By convolving the relative line intensities, given by OD, with the transmission functions of the  $V, B$  filters, and comparing the weighted, total relative line intensities inside the filters with the corresponding absolute surface intensities, obtained in a similar way as the values of Table 2, we find that for the particular nebular region: one unit of ODs' relative line intensity equals  $3 \cdot 10^{-7} \text{ erg cm}^{-2} \text{ s}^{-1} \text{ sterad}^{-1}$ . Since the calibration is made for a region inside the shell, and assuming that the nebula is optically thin, the final conversion factor is

$$\begin{aligned} \text{one unit} &= 0.5 \times 0.6 \times 3 \cdot 10^{-7} \\ &= 9 \cdot 10^{-8} \text{ erg cm}^{-2} \text{ s}^{-1} \text{ sterad}^{-1} \end{aligned} \quad (2)$$

of relative line intensity (OD), where we considered the optical path length effect by introducing  $J(D=0)/J(\text{shell}) = 0.6$ . The factor 0.5 is due to the fact that for an optically thin shell at the center of the nebula ( $D=0$ ) one observes radiation coming from two surfaces, i.e. the outer front surface and the inner rear surface. The conversion factor, and further related quantities, are accurate up to a factor 2–3. Using the conversion factor (2), the absolute surface intensities of the lines observed by OD (their Table 1) are easily calculated.

In Table 3 we give the  $H_\alpha$  and  $H_\beta$  surface emittance and surface luminosity; the luminosity is obtained by multiplying the surface emittance with the surface area of a spherical shell of  $R=8$  pc and a filling factor 1/3. For comparison we give also the  $H_\alpha$  surface emittance and surface luminosity of the Cygnus Loop as determined by Parker (1964).

Furthermore, from the relative line intensities given by OD and the conversion factor (2), we obtain for the spectral region 3727–6731 Å:

$$\begin{aligned} \text{Surface emittance:} & \quad 1.8 \cdot 10^{-4} \text{ erg cm}^{-2} \text{ s}^{-1} \\ \text{Luminosity:} & \quad 4.6 \cdot 10^{35} \text{ erg s}^{-1} \\ (R=8 \text{ pc, filling factor } 1/3) \\ \text{Volume emissivity:} & \quad 3.1 \cdot 10^{-22} \text{ erg cm}^{-3} \text{ s}^{-1} \\ (R=8 \text{ pc, } r=4 \text{ pc, homogeneous shell, filling factor } 1/3). \end{aligned}$$

For the emitted radio power the corresponding values are (WM 1966):

$$\begin{aligned} \text{Surface radio power:} & \quad 1.6 \cdot 10^{-5} \text{ erg cm}^{-2} \text{ s}^{-1} \\ \text{Radio power:} & \quad 1.2 \cdot 10^{35} \text{ erg s}^{-1} \\ \text{Radio emissivity:} & \quad 2.4 \cdot 10^{-23} \text{ erg cm}^{-3} \text{ s}^{-1} \\ (R=8 \text{ pc, homogeneous spherical shell}). \end{aligned}$$

#### IV. Comparison with Shock Wave Models (N 49)

Since no central star is detected inside N 49 (WM 1966), and since the optical spectra do not show any continuum (WM, Danziger and Dennefeld, 1976), photo ionization and photo excitation is excluded.

OD have shown that the comparison of observed line ratios with theoretical line ratios confirms, though not in all details, Cox's (1972) model by which the gas of the SNR is heated by a shock wave so that the atoms are ionized, with subsequent emission by recombination. As shown by Poveda and Woltjer (1968), and Cox (1972), the contribution by collisional excitation is small, of the order of a few percent, and therefore can be neglected.

Following a suggestion by Dr. M. A. Dopita [private communication, Equations (3)–(6); Dopita, 1976], the observed surface intensity of the  $H_\beta$  line, i.e.  $9 \cdot 10^{-6} \text{ erg cm}^{-2} \text{ s}^{-1} \text{ sterad}^{-1}$  (Table 3), enables us, by applying the theory of shock wave excitation, to derive the pre-shock interstellar density near N 49. The observed expansion velocity of the shell (MC 1973a) indicates a shock velocity  $v=200 \text{ km s}^{-1}$  which, inserted into Equation (3),

$$(v/100 \text{ km s}^{-1}) = 0.815(T/10^5 \text{ }^\circ\text{K})^{1/2} \quad (3)$$

**Table 2.** Surface intensities ( $\text{erg cm}^{-2} \text{ s}^{-1} \text{ sterad}^{-1}$ ) of N 49 and N 63 A for the Walraven five-colour pass bands

Pass band (Center wavelength Å)	Object	
	N 49	N 63 A
V (5467)	5.0 (–6)	1.1 (–5)
B (4325)	1.4 (–6)	7.9 (–6)
L (3838)	4.6 (–6)	1.6 (–5)
U (3633)	2.1 (–6)	8.4 (–6)
W(3255)	3.7 (–7)	2.5 (–6)

$$X(Y) = X \cdot 10^Y$$

**Table 3.**  $H_\alpha$ ,  $H_\beta$  surface emittance ( $\text{erg cm}^{-2} \text{ s}^{-1}$ ) and surface luminosity ( $\text{erg s}^{-1}$ ) of N 49 and the Cygnus Loop (Parker, 1964)

	N 49		Cygnus loop
	$H_\alpha$	$H_\beta$	$H_\alpha$
Surface Emittance	$9.0 \cdot 10^{-6}$	$2.7 \cdot 10^{-5}$	$1.7 \cdot 10^{-9}$
Luminosity	$2.3 \cdot 10^{34}$	$6.9 \cdot 10^{34}$	$1.2 \cdot 10^{35}$

yields a post-shock temperature  $T=6 \cdot 10^5 \text{ }^\circ\text{K}$ . Equation (4) relates the intensity of the  $H_\beta$  line,  $J(H_\beta)$ , to the post-shock temperature and the pre-shock density  $n_0$  (atoms  $\text{cm}^{-3}$ )

$$J(H_\beta) = 2.8 \cdot 10^{-7} \cdot n_0(T/10^5 \text{ }^\circ\text{K})^{1/2} \text{ erg cm}^{-2} \text{ s}^{-1} \text{ sterad}^{-1} \quad (4)$$

from which, by inserting  $J(H_\beta)$  and  $T$ , we obtain  $n_0=13$ . This value  $n_0$  may be too low by a factor  $\approx 3$  because  $J(H_\beta)$  may be a factor  $\approx 3$  higher than given in Equation (2), since in case only a filament of the shock front (shell) is observed by us, the correction factor 0.50.6 [Eq. (2)] need not to be applied. The corresponding values, obtained from a model best fitting the line ratio data, are (Dopita, 1976):  $v=67 \text{ km s}^{-1}$ ,  $T=7 \cdot 10^4 \text{ }^\circ\text{K}$ ,  $n_0=100$ . The validity of the post-shock temperature and pre-shock density derived here, can be checked in the following way: for a strong shock, in the absence of an appreciable magnetic field, the post-shock density  $n=4n_0$  (Cox, 1972), and the density of the region emitting the [S II] lines is

$$n_{[\text{S II}]} = 4n_0(T/T_{[\text{S II}]}) \quad (5)$$

where  $T_{[\text{S II}]}$  is the mean temperature of the [S II] emitting region,  $T_{[\text{S II}]}$  is typically of the order  $10^4 \text{ }^\circ\text{K}$ . Therefore, we obtain  $n_{[\text{S II}]} \approx 3 \cdot 10^3 \text{ cm}^{-3}$  which agrees well with the value  $1.2 \cdot 10^3 \text{ cm}^{-3}$  derived by OD from the [S II] line ratios.

The density  $n_0=13$  is considerably higher than the interstellar hydrogen density of the LMC,  $n(\text{H I}) \approx 2.5 \text{ atoms cm}^{-3}$ , obtained from radio observations (McGee and Milton, 1964), however,  $n(\text{H I})$  gives an average through the thickness of the LMC.

The shock thickness  $d$  is given by

$$d \approx 4 \cdot 10^{16} (T/10^5 \text{ }^\circ\text{K})^2 n_0^{-1} \quad (6)$$

which, with  $T = 6 \cdot 10^5$ ,  $n_0 = 13$ , yields  $d \approx 1 \cdot 10^{17}$  cm, or by applying the factor 3 of the uncertainty in  $J(\text{H}_\beta)$ ,  $d \approx 10^{16}$  cm, a value comparable with that given by Dopita (1976).

Since the shock theory, under the condition of a weak magnetic field, gives a consistent interpretation of the observations, the magnetic energy density  $B^2/8\pi$  in the post-shock region must be lower than the kinetic energy density of the particles, i.e.  $3/2nkT$ . Inserting the values, we find  $B < 2 \cdot 10^{-4}$  Gauss which agrees well with the value  $5 \cdot 10^{-4}$  derived by WM from the radio emission of N 49. Assuming a frozen in magnetic field, the relation (Cox, 1972)  $n_0 B = n B_0$ , i.e.  $B = 4B_0$ , holds, so that the interstellar pre-shock magnetic field  $B_0 < 5 \cdot 10^{-5}$  Gauss, a value which is comparable to field strength found in our own Galaxy.

*Acknowledgement.* Dr. J. Tinbergen and Mr. J. Schafgans, Sterrewacht Leiden, contributed considerably in writing the program and performing the preliminary reductions of the observations. Dr. D. S. Mathewson, Mt. Stromlo Observatory, kindly provided the photo-

graph of Figure 3. Dr. M. A. Dopita, Mt. Stromlo and Siding Spring Observatory, outlined the astrophysical potential of our observations and considerably improved Section IV.

## References

- Allen, C.W.: 1973, *Astrophysical Quantities*, 3. ed., The Athlone Press  
 Cox, D.P.: 1972, *Astrophys. J.* **178**, 143  
 Danziger, I.J., Dennefeld, M.: 1974, *Astron. Astrophys.* **36**, 149  
 Danziger, I.J., Dennefeld, M.: 1976, *Publ. Astron. Soc. Pacific* **88**, 44  
 Dopita, M.A.: 1976, *Astrophys. J.* **209**, 395 (Paper I; Papers II and III reprints)  
 Henize, K.G.: 1956, *Astrophys. J. Suppl. Ser.* **2**, 315  
 Lub, J., Pel, J.W.: 1977, *Astron. Astrophys.* **54**, 137  
 Mathewson, D.S., Clarke, J.N.: 1973a, *Astrophys. J.* **179**, 89  
 Mathewson, D.S., Clarke, J.N.: 1973, *Astrophys. J.* **180**, 725  
 Osterbrock, D.E., Dufour, R.J.: 1973, *Astrophys. J.* **185**, 441  
 Parker, R.A.R.: 1964, *Astrophys. J.* **139**, 493  
 Poveda, A., Woltjer, L.: 1968, *Astrophys. J.* **73**, 65  
 Rijn, R., Tinbergen, J., Walraven, Th.: 1969, *Bull. Astron. Inst. Neth.* **20**, 279  
 Rosendahl, J.D., Snowden, M.S.: 1971, *Astrophys. J.* **169**, 281  
 van Genderen, A.M.: 1974, *Inform. Bull. Var. Stars*, No. 877  
 Walraven, Th., Walraven, J.H.: 1960, *Bull. Astron. Inst. Neth.* **15**, 67  
 Walraven, Th., Walraven, J.H.: 1971, *The Magellanic Clouds 117*, ed. A. B. Muller, Reidel Publ. Co.  
 Westerlund, B.E., Mathewson, D.S.: 1966, *Monthly Notices Roy. Astron. Soc.* **131**, 371